TEXAS TECH UNIVERSITY
Libraries™

Effects of 3-week total meal replacement vs. typical food-based diet on human brain functional magnetic resonance imaging food-cue reactivity and functional connectivity in people with obesity

Appetite 120 (2018) 431–441

Contents lists available at ScienceDirect

Appetite

journal homepage: www.elsevier.com/locate/appet

Effects of 3-week total meal replacement vs. typical food-based diet on human brain functional magnetic resonance imaging food-cue reactivity and functional connectivity in people with obesity

Chanaka Nadeeshan Kahathuduwa [a, b, c], Tyler Davis [d], Michael O'Boyle [c, e], Lori Ann Boyd [a], Shao-Hua Chin [a], Dmitrii Paniukov [d], Martin Binks [a, *]

[a] Behavioral Medicine and Translational Research Lab, Department of Nutritional Sciences, Texas Tech University, Lubbock, TX, USA
[b] Department of Physiology, Faculty of Medicine, University of Peradeniya, Sri Lanka
[c] Department of Human Development and Family Studies, Texas Tech University, Lubbock, TX, USA
[d] Department of Psychological Sciences, Texas Tech University, Lubbock, TX, USA
[e] Department of Pharmacology and Neuroscience, School of Medicine, Texas Tech University Health Sciences Center, Lubbock, TX, USA

ARTICLE INFO

Article history:
Received 26 May 2017
Received in revised form
5 September 2017
Accepted 22 September 2017
Available online 25 September 2017

Keywords:
Total meal replacement
fMRI
Food-cue reactivity
Calorie restriction
Weight loss
Food cravings
Diet
Brain
Obesity

ABSTRACT

Objectives: Calorie restriction via total meal replacement (TMR) results in greater reduction of food cravings compared to reduced-calorie typical diet (TD). Direct evidence of the impact of these interventions on human brain fMRI food-cue reactivity (fMRI-FCR) and functional connectivity is absent. We examined the effects of a 3-week 1120 kcal/d TMR intervention as compared to an iso-caloric TD intervention using an fMRI-FCR paradigm.

Methods: Thirty-two male and female subjects with obesity (19–60 years; 30–39.9 kg/m^2) participated in a randomized two-group repeated measures dietary intervention study consisting of 1120 kcal/d from either 1) TMR (shakes), 2) TD (portion control). Pre-intervention and following the 3-week diet fMRI-FCR, functional connectivity, food cravings (Food Craving Inventory) and weight were considered.

Results: Compared to TD, TMR showed increased fMRI-FCR of the bilateral dorsolateral prefrontal (dlPFC), orbitofrontal, anterior cingulate, primary motor and left insular cortices and bilateral nucleus accumbens regions in the post-intervention state relative to the pre-intervention state. Compared to TD, TMR was also associated with negative modulation of fMRI-FCR of the nucleus accumbens, orbitofrontal cortex and amygdala by dlPFC. Reduced body weight (4.87 kg, $P < 0.001$), body fat (2.19 kg, $P = 0.004$) and overall food cravings (0.41, $P = 0.047$) were seen in the TMR group. In the TD group reduced body weight (2.37 kg, $P = 0.004$) and body fat (1.64 kg, $P = 0.002$) were noted. Weight loss was significantly greater in TMR versus TD (2.50 kg, $P = 0.007$).

Conclusions: Greater weight loss and reduced cravings, coupled with stronger activations and potential negative modulation of the food reward related regions by the dlPFC during exposure to visual food cues is consistent with increased executive control in TMR vs. TD.

1. Introduction

Prevalence of over-weight and obesity are rising worldwide (Ng et al., 2014). Extended calorie restriction (ECR) is often used for weight loss (Finer, 2001; Franz et al., 2007). Several studies have described reduced food cravings and food-related reward expectancy following ECR (Harvey, Wing, & Mullen, 1993; Martin, O'Neil, & Pawlow, 2006, 2011). Moreover, it has been demonstrated that ECR via liquid formula-based total meal replacement (TMR) very low-calorie diet suppresses food cravings to a greater extent compared to ECR via a typical food-based low-calorie diet (TD) (Martin et al., 2006).

Our recent review (Kahathuduwa, Boyd, Davis, O'Boyle, & Binks, 2016), noted there is little research directly examining human brain functional magnetic resonance imaging food-cue reactivity (fMRI-FCR) involving ECR, as most studies focus on total fasting (typically

* Corresponding author. Department of Nutritional Sciences, College of Human Sciences, Texas, Tech University, 1301 Akron Street, Box 1270, Lubbock, TX 79409-1270, USA.
E-mail address: m.binks@ttu.edu (M. Binks).

https://doi.org/10.1016/j.appet.2017.09.025

List of abbreviations

ACC	anterior cingulate cortex
BF	body fat
BL	baseline of fMRI signal
COPEs	contrasts of parameter estimates
dlPFC	dorsolateral prefrontal cortex
ECR	extended calorie restriction
FCI	Food Craving Inventory
fMRI	functional magnetic resonance imaging
FSL	FMRIB Software Library
NAcc	nucleus accumbens
NS	not significant
OFC	orbitofrontal cortex
PCG	precentral gyrus
ROIs	regions of interest
TMR	total meal replacement
TD	typical diet
VAS	visual analogue scales
vmPFC	ventromedial prefrontal cortex

24–48 h). Evidence suggests that ECR may be associated with decreased food-cue reactivity in brain regions regulating energy balance (e.g. hypothalamus (Rosenbaum, Sy, Pavlovich, Leibel, & Hirsch, 2008)), some regions of the dopaminergic reward system (e.g. orbitofrontal cortex (Bruce et al., 2014; Rosenbaum et al., 2008), anterior cingulate cortex (Murdaugh, Cox, Cook, & Weller, 2012; Rosenbaum et al., 2008) amygdala (Rosenbaum et al., 2008)), nucleus accumbens (Avena, Murray, & Gold, 2013) and regions that execute ingestive behavior (e.g. precentral gyrus (Rosenbaum et al., 2008)). This decrease in reactivity in the dopaminergic reward system, homeostatic regions, and regions associated with ingestion from ECR is frequently accompanied by increased activation in the middle frontal gyrus (i.e. dorsolateral prefrontal cortex) (Rosenbaum et al., 2008). This has been interpreted as indicating greater executive control over ingestion and food cravings.

However, several gaps in understanding of the neurophysiological and behavioral effects of ECR remain. First, changes in fMRI-FCR in the context of ECR have not been prospectively examined in a randomized controlled trial (Kahathuduwa et al., 2016). Second, even though evidence suggests that ECR suppresses food cravings and fMRI-FCR in several brain regions that process food-related stimuli and reward, the precise nature of the neurophysiological mechanisms involved are unknown. Third, exploring functional connectivity using psychophysiological interaction (PPI) analysis could lead to the identification of potential mechanisms linking brain regions that are associated with decreased food cravings observed in relation to ECR. While the dorsolateral prefrontal cortex has often been assumed to be exerting executive control over ingestion, the effects of ECR-associated suppressive relationships between the dorsolateral prefrontal cortex and the reward-related brain regions have not been studied to-date. Finally, even though previous evidence suggested that a very low-calorie diet implemented via liquid formula-based TMR seems to be superior to a low-calorie diet implemented via TD in suppressing food cravings, effects of these interventions on food cravings, fMRI-FCR and functional connectivity between the dorsolateral prefrontal cortex and the food reward-related regions of the brain have not been delineated in a randomized controlled trial.

Therefore, we examined whether participation by subjects with obesity (BMI 30–39.9 kg/m^2) in a 3-week isocaloric, low calorie (1120 kcal/day) diet derived from TMR versus TD will have differential effects on functional activations (i.e. BOLD responses) in brain regions that influence ingestive behavior. We hypothesized that a significant group (i.e. TMR versus TD) X time (i.e. pre- vs. post-intervention) interaction and a significant main effect for time would be seen in the fMRI-FCR of the brain regions that are thought to regulate executive control over ingestion (i.e. dorsolateral prefrontal cortex) and brain regions that have been associated with food reward (i.e. orbitofrontal cortex, anterior cingulate cortex, amygdala, precentral gyrus and the nucleus accumbens). While direct evidence was not available regarding the possible role of the insula in fMRI-FCR, considering that one of its functions includes regulating pleasure associated with ingestion (Berridge, 2009), we anticipated that the fMRI-FCR of the insula would also decrease with ECR as would other food reward and pleasure-related regions (Kahathuduwa et al., 2016). We specifically hypothesized *a priori*, an increase in fMRI-FCR compared to pre-intervention state in the dorsolateral prefrontal cortex in both groups, with fMRI-FCR of the TMR group being greater than the TD group. We also predicted a decline in fMRI-FCR in all hypothesized food reward, and pleasure-related regions and brain regions that regulate motor readiness to ingest, with a greater decline in TMR versus TD. In relation to the functional connectivity analyses, we hypothesized that in a post- vs. pre-intervention comparison, the fMRI-FCR of bilateral dorsolateral prefrontal cortices will be negatively associated with fMRI-FCR of the brain regions that regulate food reward (i.e. bilateral nucleus accumbens, orbitofrontal cortex, insula, amygdala and anterior cingulate cortex) and motor responses in relation to ingestion (i.e. the precentral gyrus) 1) in the TMR group when compared with the TD group; and 2) in a pooled analysis of TMR and TD groups (i.e. independent influence of ECR). Finally, with regard to self-reported food cravings, we hypothesized that compared to TD, TMR would be associated with a significant reduction of overall food cravings as well as cravings for sweet food, high-fat food, starchy food and fast food as measured by the Food Craving Inventory (White, Whisenhunt, Williamson, Greenway, & Netemeyer, 2002).

2. Methods

2.1. Ethics

The TTU Human Research Protection Program approved the study (TTU IRB #505380). All procedures were conducted in accordance with the Helsinki Declaration amended in 2000 (WHO, 2001). Informed written consent was obtained from all subjects who met eligibility criteria.

2.2. Subjects

Thirty-two adult men and women with obesity (age 19–60 years; BMI 30–39.9 kg/m^2) were enrolled from January through June 2016. Potential subjects were screened to determine eligibility via telephone. Subjects were excluded based on the following: contraindications for magnetic resonance imaging; gross visual, auditory or motor impairments; medical contraindications (e.g. diabetes mellitus, uncontrolled hypertension), neurological or severe psychiatric conditions; recent (3 months) weight loss program or ever had bariatric surgery; diagnosed eating disorders; taking medications that may affect fMRI-FCR; current smokers; and unwilling to undergo a 3-week diet. Eligible subjects attended an in-person assessment (visit 1). Pre-menopausal women were scheduled for visit 2 during the second half of the follicular phase of their menstrual cycle (i.e. day 10–14). This allowed for scheduling visit 5 within the follicular phase of the subsequent menstrual cycle (i.e.

approximately day 3–7) to avoid menstrual influences on fMRI-FCR (Berridge, 2009).

2.3. Design

We employed a two-group repeated-measures design. During visit 1, subjects' eligibility was confirmed using a self-report questionnaire. Height and weight were measured and BMI calculated. Body fat mass (BF) was obtained via bio-electrical impedance analysis (TANITA Corporation of America Inc., IL, USA BC-418 segmental body composition analyzer); and blood pressure measured (Omron Healthcare Inc., IL, USA Digital BP Monitor HEM-907XL). Once eligibility was verified, visits 2–5 were scheduled [see Supplemental Fig. 1].

2.3.1. fMRI and check-in visits

In preparation for each scanning visit (visit 2 and 5), subjects were instructed to refrain from alcohol, caffeine, and tobacco for 24 h and to avoid intake of food or beverages (except water) for 8 hours. Upon arrival for scanning visits, subjects completed self-report measures including the Food Craving Inventory (White et al., 2002) and Visual Analogue Scales [Fig. 1]. The Food Craving Inventory is validated 28-item self-report questionnaire that measures overall food cravings and cravings for sweet food, high-fat food, starchy food and fast food. The inventory requires subjects to rate the frequency of development of cravings to each item of food within the past 3 months on a 1–5 Likert scale. Validation studies report that the Food Craving Inventory has reasonable internal consistency (Cronbach's α = 0.76–0.93) and test-re-test reliability of 0.79–0.91. Cronbach's α for this study is reported in Supplemental Table 1. The Visual Analogue Scales required the subjects to rate hunger, satiety, thirst, fullness and emptiness on a 0–100 mm scale. The Visual Analogue Scales were administered twice at each scanning session (i.e. once before and once immediately after the scanning session). Within each scanning session, the mean of the two administrations was tabulated.

Upon completion of the self-report measures, subjects were oriented to the fMRI stimulus presentation paradigm using a laptop computer prior to undergoing a 45-min fMRI scan. After completion of the scan, the 5 Visual Analogue Scales were re-administered. Following the pre-intervention scan, subjects were randomly assigned to diet condition (TMR n = 16 or TD n = 16) using a random number generator (Team, 2016). The TMR group was instructed to maintain calorie intake at 1120 kcal/day by consuming provided Optifast™ 800 (Nestlé HealthCare Nutrition Inc., NJ, USA) TMR shakes and non-caloric beverages for 3 weeks. Each subject was provided with 49 sachets (170 kcal/sachet) of TMR formula per week; were instructed to consume 7 sachets per day at regularly spaced times of their own discretion (per typical clinical recommendations they were instructed they could double up shakes if desired). Subjects were instructed to record the times of consumption and the number of sachets consumed at each time. The TD group was instructed to maintain calorie intake at 1120 kcal/day for 3 weeks by controlling portion sizes and calorie monitoring (2016 Calorie Fat & Carbohydrate Counter, The Calorie King®; CA, USA) foods they typically eat. No specific dietary recommendations were made. The TD group also recorded the times of intake of food and the number of calories that were consumed at each occasion in order to improve adherence. Both TMR and TD groups were instructed to maintain their physical activity at a constant level throughout the 3-week intervention.

Subjects in both groups were weighed, blood pressure measured and adherence encouraged by providing constructive feedback related to adherence of the prior week at weekly check-in visits. An identical protocol to visit 2 was used for visit 5 scan at completion of the 3-week intervention. Measured height, body weight, BF and BMI were also obtained (see visit 1).

2.4. Imaging paradigm

Scanning sessions were conducted using a 3.0 T S Skyra scanner (with a 20-channel head coil). Subjects underwent event-related stimulus paradigm (PsychoPy 2.0) fMRI scans followed by a diffusion tensor imaging (dTI) scan (data reported elsewhere) and a T1-weighted structural scan. We used pairs of high-resolution (food/object) images that were matched for visual properties (color,

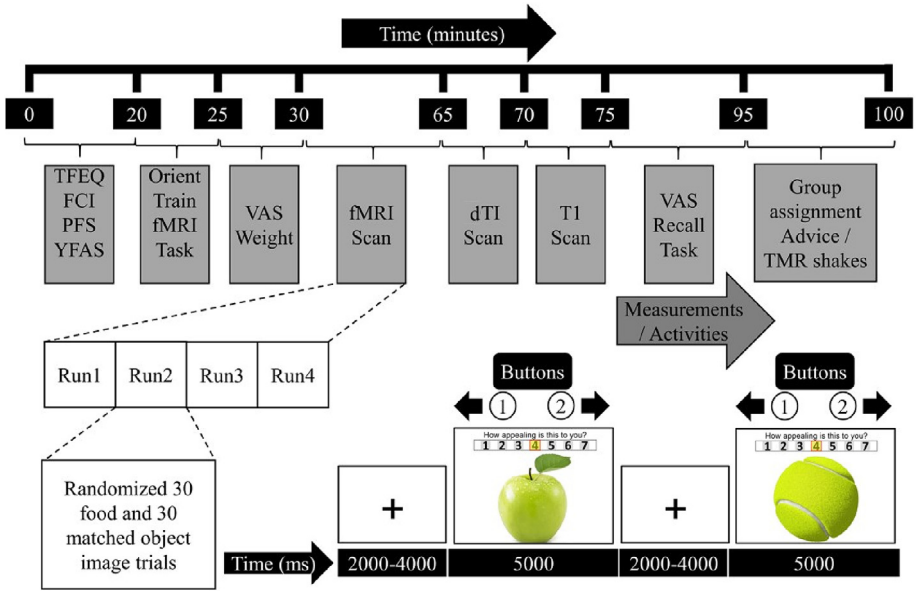

Fig. 1. Protocol followed during scanning sessions.
The protocol was followed during visit 2 and visit 5. Only a sample food image and the matched control image are shown. TFEQ, Three-factor Eating Questionnaire; FCI, Food Craving Inventory; PFS, Power of Food Scale; YFAS, Yale Food Addiction Scale; VAS, visual analogue scales; DTI, diffusion tensor imaging; TMR, total meal replacement.

shape visual complexity, orientation and size) by 3 independent raters to create the image bank. The images of food included images ranging from high to low energy density and both food and matched object images ranged from high to low appeal (confirmed via independent online validation survey of 110 subjects who rated each image on a 0–100 visual analogue scale). Each fMRI trial included a black fixation cross displayed on a white background for a jittered duration between 2000 and 4000 ms and subsequently a target image (i.e. food or object) displayed for 5000 ms. Subjects were asked to rate the image on a 1–7 Likert scale by answering 'How appealing is this to you?' during image presentation using a two-button fiber-optic device held in the right hand. Each run consisted of repeating this sequence 60 times (i.e. 30 images of food and 30 images of matched objects). Each functional scanning session was made up of 4 runs, thus presenting 120 images from each of the food and object categories. Both the order of presentation of images within each pre-determined 60-image run and the order of presentation of the runs were randomized.

fMRI data were acquired using an echo planar imaging sequence with the following parameter settings: repetition time = 2140 ms; echo time = 25; flip angle = 70; field of view = 192 mm × 192 mm; acquisition matrix = 64 × 64; slice thickness = 2.5 mm; and 42 ascending axial slices. Slices were tilted approximately 30° from the anterior commissure – posterior commissure line to minimize orbitofrontal cortical signal dropout (Deichmann, Gottfried, Hutton, & Turner, 2003). A T1-weighted MPRAGE scan was also collected using the following parameters: repetition time = 1900 ms; echo time = 2.49; flip angle = 9; field of view = 240 × 240; acquisition matrix = 256 × 256; slice thickness = 0.9 mm; and 192 slices in the sagittal plane. Each scanning session was completed within 45 minutes.

2.5. Statistical analysis

2.5.1. Behavioral data analyses

All behavioral data analyses were conducted using R statistical software (version 3.2.4). All continuous variables were summarized using means and standard deviations. Student's t-test with Welch–Satterthwaite correction and Yates continuity corrected chi-square test were used to compare the behavioral measurements across groups at the pre-intervention state. Pre- and post-intervention differences were calculated for each behavioral measure within groups. Change scores for groups were compared using Student's t-tests with Welch–Satterthwaite correction. P-value of < 0.05 was considered significant.

2.5.2. Functional MRI data analyses

All structural and functional raw data images were converted to NIfTI format using the dcm2nii converter (Rorden & Brett, 2000). Freesurfer (autorecon1) (Dale, Fischl, & Sereno, 1999; Fischl et al., 2004) was used for structural image preprocessing and FMRIB Software Library (FSL; Version 6.00, Oxford, UK) for functional image preprocessing and analysis. Preprocessing of functional images included: motion correction by aligning each functional volume to the center volume within each functional run with 6-DOF sinc interpolation using FSL's MCFLIRT tool (Jenkinson, Bannister, Brady, & Smith, 2002); skull-stripping using FSL's BET tool (Smith, 2002); registration to high resolution structural space by the BBR algorithm and subsequently to the standard space by 12-DOF using FSL's FLIRT tool (Jenkinson & Smith, 2001); spatial smoothing using a Gaussian kernel of FWHM 8.0 mm; grand-mean intensity normalization of the entire 4D dataset by a single multiplicative factor; high-pass temporal filtering (Gaussian-weighted least-squares straight line fitting, with sigma = 50.0 s); and FILM pre-whitening (Woolrich, Ripley, Brady, & Smith, 2001).

Standard 3-level analysis in the FEAT tool in FSL was used to analyze fMRI data. In level-1 models, single run functional time series were modeled with task-based regressors for food and object stimuli, and trials where subjects did not make a motor response. Task-based regressors were convolved using a canonical double gamma hemodynamic response function. Confound variables to control for motion effects included 6 motion parameters, their temporal derivatives, and regressors to scrub (i.e. censor) volumes that exceeded a frame-wise displacement of 0.9 mm. An autocorrelation correction was included to account for serial dependencies between samples not accounted for by the task and confound variables. In the level-2 analyses, the level-1 experimental variables of all functional runs of each subject were averaged using a fixed effects model (Beckmann, Jenkinson, & Smith, 2003; Woolrich, 2008; Woolrich, Behrens, Beckmann, Jenkinson, & Smith, 2004), including a variable accounting for pre- versus post-intervention effects. In the third level analysis, level-2 averages and contrasts were regressed on the grouping variable (TMR vs. TD) and two covariates determined *a priori*: 1) standardized difference in duration of fasting pre-scan (to control for known influences of duration of fasting (Kahathuduwa et al., 2016)); 2) standardized change in fat mass (BF) relative to the pre-intervention state to control for potential systematic bias caused by between group differences in response and or adherence to diet, using a mixed effects model with subject as a random effect for population inference (FLAME 1). The final statistical maps were corrected for multiple comparisons at $P < 0.05$ using FSL's permutation-based cluster thresholding (randomise; 10,000 permutations; 2.0555 t-threshold corresponding to the two-tailed t-threshold of 26 degrees of freedom at the significance level of 0.05). Harvard-Oxford cortical and subcortical structural atlases and FSL's atlasquery tool were used to identify the brain regions showing statistical significance. In addition to whole-brain thresholds, small-volume corrected analyses were conducted using probability masks derived from the Harvard-Oxford cortical and subcortical structural atlases for the following *a priori* regions of interest (ROIs): bilateral dorsolateral prefrontal cortex, orbitofrontal cortex, anterior cingulate cortex, nucleus accumbens, insula, amygdala, and precentral gyrus. A separate level 3 analysis, including the same covariates and pooling the TMR and TD groups, at the whole brain level and using the probability masks of the pre-hypothesized ROIs to examine for the main effect of time (i.e. pre- vs. post-intervention) was also conducted. Each statistical image of ROI analysis was corrected for multiple comparisons at $P < 0.05$ using FSL's permutation-based cluster thresholding as described above.

2.5.3. Functional connectivity analyses

Probability masks of each of left and right dorsolateral prefrontal cortices (i.e. seed regions), defined using the left and right middle frontal gyrus masks of the Harvard-Oxford cortical structural atlas in FSL, were converted to the functional space of each functional run of each subject using the FNIRT tool in FSL (Andersson, Jenkinson, & Smith, 2007). Time-course of each seed region was extracted from the pre-processed data using the fslmeants command in FSL.

Two standard 3-level analyses in the FEAT tool in FSL were used to analyze the functional connectivity data for the two seed regions (i.e. the left and right dorsolateral prefrontal cortex) using the PPI approach as per FSL's standard PPI analysis pipeline (https://fsl.fmrib.ox.ac.uk/fsl/fslwiki/PPI). In level-1 models, single run functional time series were modeled with a 3-column (i.e. time of onset of each trial, duration of each trial and weight of each trial) task-based regressor with weights coded to depict the food – object image contrast were high-pass filtered and were convolved using a canonical double gamma hemodynamic response function (i.e. the

psychological regressor). The non-convolved time course of the seed region (i.e. the physiological regressor) was also included in the model. The interaction of the centered psychological and the mean centered physiological regressors (i.e. the PPI) was also modeled. A 3-column high-pass filtered and convolved (using a canonical double gamma hemodynamic response function) task-based regressor that depicted the food + object image contrast (i.e. all images having the same weights) was also included in the models as a covariate. The trials in which subjects did not make a motor response were included in the model as confounding variables. Additional confound variables to control for motion effects included the 6 motion parameters, their temporal derivatives, and regressors to scrub (i.e. censor) volumes that exceeded a frame-wise displacement of 0.9 mm (Siegel et al., 2014). Level 2 and level 3 analyses, subsequent thresholding, localizing and ROI analyses were conducted as described above.

3. Results

Fifteen subjects in the TMR group and 13 subjects in the TD group completed the study [see Supplemental Fig. 2: CONSORT diagram] and were included in the analyses. The two groups did not differ by age, sex, proportion of pre- versus post-menopausal women, weight, height, BMI, BF or food cravings [Table 1]. Non-completers did not differ statistically from completers at the pre-intervention state.

The 3-week TMR intervention resulted in a significant reduction in overall food cravings (0.41, t = 2.18, P = 0.047, Cohen's d = 0.56), cravings for sweets (0.68, t = 2.56, P = 0.023, Cohen's d = 0.66) and for starchy food (0.44, t = 2.15, P = 0.049, Cohen's d = 0.55). The TD intervention also resulted in a significant reduction in cravings for sweets (0.37, t = 2.26, P = 0.043, Cohen's d = 0.62) and cravings for starchy food (0.38, t = 2.52, P = 0.027, Cohen's d = 0.70) [Table 2].

In the fMRI-FCR analyses, TMR and TD groups were compared for post- versus pre-intervention differences in responses to images of food versus objects both at the whole brain level and in pre-hypothesized ROIs. Whole brain level analysis comparing the TD group, to the TMR group showed increased fMRI-FCR in a cluster that included the bilateral orbitofrontal, dorsolateral prefrontal, anterior cingulate and the left insular cortices and the bilateral precentral gyri in the post-intervention state relative to the pre-intervention state, as evidenced by a significant TMR > TD X post- > pre-intervention X food > object stimulus interaction observed after cluster-based correction for multiple comparisons (P = 0.043) [Fig. 2; Supplemental Table 2]. Breaking down this three-way interaction revealed increased fMRI-FCR of the above brain regions in the TMR group compared to the TD group post-intervention relative to baseline of fMRI signal (P = 0.010) (i.e. a significant TMR > TD X post-intervention > baseline of fMRI signal X food > object contrast). The TMR versus TD contrast however, was not significant in baseline of fMRI signal versus pre-intervention contrast. Examination of main effect for time (post- versus pre-intervention) did not reveal significant results at the whole brain level. This may be due to the mean of increased post-intervention fMRI-FCR in the TMR group and the decreased post-intervention fMRI-FCR of the TD group, approximating the pre-intervention fMRI-FCR of the two groups. Taken together, the whole brain-level analyses indicated that compared to the TD group, the TMR group had increased fMRI-FCR in the bilateral dorsolateral prefrontal cortices, which are thought to exert executive inhibitory control over ingestion (Berthoud, 2002, 2004, 2011), and also in the food-reward-related bilateral orbitofrontal, anterior cingulate and left insular regions (Berridge, 2009; Berthoud, 2002, 2011) and bilateral precentral gyri, which regulates motor readiness to ingest (Kahathuduwa et al., 2016).

ROI analyses revealed that compared to the TD group, the TMR group had increased fMRI-FCR post-intervention relative to pre-intervention in the right and left dorsolateral prefrontal (P = 0.017 and 0.042), orbitofrontal (P = 0.027 and 0.017) and anterior cingulate (P = 0.014) cortices and the bilateral nucleus accumbens (P = 0.038 and 0.035) (i.e. TMR > TD X post- > pre-intervention X food > object stimulus interactions in each ROI) after cluster-based correction for multiple comparisons [Table 3]. On subsequent analyses, compared to the TD group, in the TMR group, significantly increased fMRI-FCR was observed post-intervention relative to baseline of the fMRI signal in all of the above ROIs. Visual examination of contrasts of parameter estimates (COPEs) derived from each brain ROI for the TMR and TD groups in the pre- and post-intervention states [Supplemental Fig. 3] revealed that TMR was associated with increased fMRI-FCR in the bilateral

Table 1
Pre-intervention characteristics of completers of the study.

Parameter	TMR (n = 15) [a]	TD (n = 13) [a]	t/χ2	Cohen's d	P
Age (years)	31.27 ± 11.85	32.15 ± 14.67	−0.188	0.067	0.861
Gender (M/F)	8/7	4/9	0.673		0.412
Reproductive status of women (pre-/post-menopausal)	4/3	6/3	0.000		>0.999
Weight (kg)	97.97 ± 16.72	100.06 ± 16.70	−0.355	0.125	0.725
Height (cm)	166.67 ± 9.74	169.11 ± 12.66	−0.611	0.216	0.546
BMI (kg/m^2)	35.14 ± 3.75	34.82 ± 2.63	0.283	0.1	0.779
BF (kg)	38.03 ± 13.32	40.28 ± 6.18	−0.613	0.217	0.545
BF %	38.65 ± 11.48	40.95 ± 7.19	−0.679	0.24	0.502
Food cravings – Overall	2.44 ± 0.57	2.36 ± 0.61	0.399	0.141	0.692
Food cravings – Sweet	2.83 ± 0.74	2.76 ± 0.99	0.238	0.084	0.813
Food cravings – High Fat	2.02 ± 0.61	1.93 ± 0.50	0.427	0.151	0.673
Food cravings - Starchy	2.53 ± 0.62	2.48 ± 0.78	0.210	0.074	0.835
Food cravings – Fast Food	2.98 ± 1.01	2.3 ± 0.86	0.760	0.269	0.453
Fasting (hours) [b]	13.51 ± 3.96	14.37 ± 5.16	−0.527	0.186	0.602
VAS-Hunger	44.37 ± 18.96	50.65 ± 25.88	−0.724	0.193	0.477
VAS-Satiety	46.15 ± 23.41	49.15 ± 22.24	−0.348	0.093	0.731
VAS-Thirst	55.15 ± 26.10	56.75 ± 27.06	−0.159	0.042	0.875
VAS-Fullness	30.03 ± 16.29	34.73 ± 23.33	−0.609	0.163	0.549
VAS-Hunger	56.15 ± 16.03	58.46 ± 21.60	−0.317	0.085	0.754

Data were analyzed with Student's t-tests with Welch–Satterthwaite correction and chi-square test with Yates continuity correction where appropriate. BF, body fat; TMR, Total Meal Replacement; TD, Typical Diet.

[a] Values are means ± SDs or ratios as appropriate.

[b] Time since the last intake of food/calorie containing beverage prior to the pre-intervention scanning session.

Table 2
Comparison of the changes in body weight, BMI, BF, BF percentage and food cravings in the TMR and TD groups during the 3-week intervention.

Parameter	TMR (n = 15) [95%CI]	TD (n = 13) [95%CI]	TMR vs. TD [95% CI]	t	Cohen's d	P
	Pre- vs. Post-	Pre- vs. Post-	Pre- vs. Post-			
Weight (kg)	4.87 [3.71, 6.02][a]	2.37 [0.93, 3.81][a]	2.50 [0.74, 2.92][b]	2.924	1.120	0.007
BMI (kg/m^2)	1.68 [1.28, 2.08][a]	0.44 [−0.45, 1.33]	1.24 [0.30, 2.19][b]	2.774	1.100	0.010
BF (kg)	2.18 [0.83, 3.54][a]	1.64 [0.75, 2.53][a]	0.54 [−1.01, 2.10]	0.723	0.265	0.477
BF %	0.60 [−0.53, 1.74]	0.68 [−0.22, 1.59]	−0.08 [−1.48, 1.31]	−0.125	0.046	0.901
FCI – Overall	0.41 [0.01, 0.80][a]	0.21 [−0.06,0.49]	0.19 [−0.27, 0.65]	0.851	0.312	0.403
FCI – Sweet	0.68 [0.11, 1.26][a]	0.37 [0.01,0.72][a]	0.32 [−0.33, 0.96]	1.018	0.371	0.319
FCI – High Fat	0.11 [−0.33, 0.54]	0.09 [−0.12,0.30]	0.02 [−0.45, 0.49]	0.097	0.035	0.924
FCI - Starchy	0.44 [0.00, 0.88][a]	0.38 [0.05, 0.72][a]	0.06 [−0.47, 0.59]	0.223	0.082	0.826
FCI – Fast Food	0.58 [−0.02, 1.19]	0.02 [−0.46, 0.50]	0.56 [−0.17, 1.30]	1.580	0.585	0.126
Fasting (hours)	−0.43 [−2.82, 1.97]	0.67 [−2.04, 3.39]	−1.10 [−0.43, 0.67]	−0.658	0.250	0.516
VAS-Hunger	−8.27 [−19.98, 3.45]	1.77 [−9.51, 13.05]	−10.04 [−25.51, 5.43]	−1.333	0.356	0.194
VAS-Satiety	1.48 [−9.15, 12.12]	−3.15 [−14.71, 8.41]	4.64 [−10.31, 19.58]	0.638	0.171	0.529
VAS-Thirst	2.08 [−15.38, 19.55]	2.17 [−14.64, 18.98]	−0.09 [−23.15, 22.97]	−0.008	0.002	0.994
VAS-Fullness	10.13 [−2.07, 22.34]	−2.42 [−12.58, 7.74]	12.56 [−2.58, 27.69]	1.706	0.456	0.100
VAS-Emptiness	−9.08 [−24.60, 6.43]	3.77 [−5.39, 12.93]	−12.85 [−30.20, 4.49]	−1.536	0.411	0.139

Pre- versus Post-intervention comparisons were conducted using paired t-tests. TMR versus TD comparisons were conducted using Student's t-tests with Welch–Satterthwaite correction. BF, body fat; TMR, Total Meal Replacement; TD, Typical Diet.
[a] Significant pre- versus post-difference.
[b] Significant TMR versus TD difference.

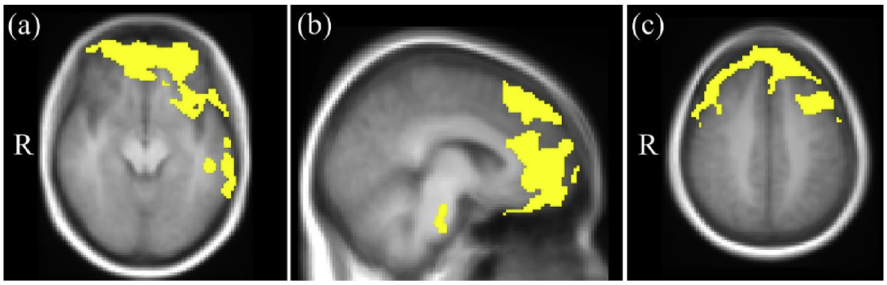

Fig. 2. Brain regions showing significant TMR > TD X post- > pre-intervention X food > object stimulus interaction on whole brain level analysis.
a) Coronal slice of the brain showing significant clusters involving bilateral dlPFC and left insular cortical regions.
b) Transverse slice of the brain showing significant clusters involving bilateral orbitofrontal and anterior cingulate cortical regions.
c) Sagittal slice of the brain showing significant clusters involving medial prefrontal, orbitofrontal and anterior cingulate cortical regions.
Analyses were conducted using FSL. Third level random effects models were constructed using the FLAME-1 algorithm in FSL. Cluster thresholding was performed via the randomise tool in FSL ($t > 2.0555$, 10000 permutations; the cluster forming threshold was the t-score corresponding to a FWER of 0.05 at 26 degrees of freedom). Only the clusters and the local maxima that survived the FWE cluster correction ($P < 0.05$) are shown. The template image is the mean image of the high-resolution anatomical scans of all subjects. TMR, Total Meal Replacement; TD, Typical Diet; OFC, orbitofrontal cortex; ACC, anterior cingulate cortex; dlPFC, dorsolateral prefrontal cortex; FSL, FMRIB Software Library.

dorsolateral prefrontal cortex, anterior cingulate cortex, nucleus accumbens, orbitofrontal cortex and the pre-central gyrus, whereas the TD intervention was associated with decreased fMRI-FCR in the above regions. Main effect of time (i.e. post- vs. pre-intervention) was not significant in any of the examined ROIs. Similar to the whole brain level analyses, ROI analyses indicated that compared to TD, TMR was associated with increased fMRI-FCR of brain regions that regulate executive inhibitory control over ingestion (i.e. the dorsolateral prefrontal cortex), as well as brain regions that may be associated with food reward (i.e. the orbitofrontal cortex) (Berthoud, 2002, 2004, 2011).

In the PPI analysis, the effects of the TMR intervention as compared to the TD intervention on the associations between activity of left and right dorsolateral prefrontal cortices on fMRI-FCR of the whole brain and in pre-hypothesized ROIs were examined. In the whole brain level analysis, we found a negative functional interaction between the time-course of the left dorsolateral prefrontal cortex and the fMRI-FCR of a cluster that included the bilateral orbitofrontal cortex, bilateral amygdala, frontal pole, bilateral parahippocampal gyri, left hippocampus, left superior temporal gyrus, left inferior temporal gyrus and the left planum temporale following the TMR intervention as compared to the TD group ($P = 0.031$) [Fig. 3, Supplemental Table 3]. This negative interaction suggested that increased activity of the left dorsolateral prefrontal cortex seems to be associated with decreased fMRI-FCR of the above brain regions following the TMR intervention as compared to the TD intervention. In similar analyses conducted using probability masks of pre-hypothesized ROIs, we found negative functional interactions between the time-course of the left dorsolateral prefrontal cortex and the fMRI-FCR of the left and right amygdala ($P = 0.004$ and $P = 0.009$ respectively), left nucleus accumbens ($P = 0.018$) and left orbitofrontal cortex ($P = 0.01$) following the TMR intervention as compared to the TD intervention [Table 4]. Further exploration of these findings indicated that observed significant findings in the bilateral amygdala and the left orbitofrontal cortex were driven by significant differences in TMR vs. TD groups in the interaction of the left dorsolateral prefrontal cortex and fMRI-FCR of these target brain regions at the pre-intervention state (rather than following the intervention). Visual examination of contrasts of parameter estimates (COPEs) extracted from the above ROIs using Harvard-Oxford probability masks confirmed this finding. However, visual examination of the mean COPEs suggested that following TMR intervention, as the activity of the left dorsolateral prefrontal cortex increased, fMRI-FCR of the

Table 3
Local maxima within pre-hypothesized ROIs in the fMRI analyses.

Contrast	ROIs	Cluster Size	MNI Coordinates			Subregions	t	P
			X	Y	Z			
TMR > TD X Post > Pre X Food > Object	OFC	530	−46	30	−8	Left lateral OFC	3.43	0.017
		391	40	22	−16	Right lateral OFC	3.83	0.027
	MFG	1132	36	28	52	Right dlPFC	3.69	0.017
			32	20	56	Right dlPFC	3.55	
			34	10	46	Right dlPFC	3.53	
			28	18	54	Right dlPFC	3.48	
			32	16	58	Right dlPFC	3.47	
		622	−44	22	48	Left dlPFC	3.64	0.042
			−50	10	50	Left dlPFC	3.4	
			−28	34	50	Left dlPFC	3.37	
			−50	24	40	Left dlPFC	3.31	
			−38	34	46	Left dlPFC	3.22	
	ACC	618	0	38	−2	Pregenual ACC	4.29	0.014
			−4	40	−2	Pregenual ACC	4.14	
			0	46	6	Pregenual ACC	3.65	
			0	30	18	Pregenual ACC	3.55	
			−8	40	18	Pregenual ACC	2.5	
	NAcc	38	−8	14	−4	Left NAcc	2.79	0.035
		35	8	8	−4	Right NAcc	2.68	0.038
	Insula	128	34	20	−8	Right anterior insula	2.75	0.083
		31	−28	16	−12	Left anterior insula	3.47	0.206
	PCG	63	54	2	46	Right primary motor cortex	2.52	0.246
		47	−60	12	34	Left primary motor cortex	2.54	0.278
	Amygdala	NS						
TD > TMR X Post > Pre X Food > Object	NS							
TMR > TD X Post > BL X Food > Objects	OFC	671	−24	18	−14	Left medial OFC	4.13	0.007
			−20	18	−22	Left medial OFC	3.71	
			−40	28	−18	Left lateral OFC	3.5	
			−42	34	−14	Left lateral OFC	3.49	
			−46	28	−10	Left lateral OFC	3.45	
		350	22	18	−20	Right medial OFC	3.65	0.032
			36	20	−24	Right lateral OFC	3.31	
			20	10	−28	Right medial OFC	2.22	
	MFG	970	−36	34	46	Left dlPFC	4.07	0.011
			−48	10	54	Left dlPFC	4.03	
			−32	34	50	Left dlPFC	3.91	
			−42	26	44	Left dlPFC	3.9	
			−42	12	56	Left dlPFC	3.88	
		606	36	6	54	Right dlPFC	4.23	0.029
			36	26	52	Right dlPFC	2.14	
			30	34	46	Right dlPFC	3.58	
			34	14	40	Right dlPFC	2.81	
			38	20	34	Right dlPFC	2.48	
	ACC	780	0	36	2	Pregenual ACC	4.17	0.005
			0	46	6	Pregenual ACC	3.67	
			0	22	18	Mid-ACC	3.47	
			−12	34	20	Left Mid-ACC	3.35	
			−4	34	20	Pregenual ACC	3.25	
	NAcc	79	−8	16	−6	Left NAcc	3.81	0.007
		60	8	6	−4	Right NAcc	3.98	0.016
	Insula	93	38	0	−18	Right NAcc	2.64	0.103
		60	−38	−12	−8	Left NAcc	2.64	0.14
	PCG	146	−60	12	34	Left primary motor cortex	3.03	0.134
		90	48	4	16	Right primary motor cortex	2.58	0.18
	Amygdala	12	32	−4	−24	Right amygdala	2.39	0.157
		6	−22	−14	−12	Left primary motor cortex	2.41	0.198
TMR > TD X BL > Pre X Food > Objects	NS							
TMR > BL X Post > BL X Food > Objects	NS							
BL > TD X Post > BL X Food > Objects	NS							

Fifteen TMR and 13 TD subjects were included in the analyses. Analyses were conducted using FSL. Third level random effects models were constructed using the FLAME-1 algorithm in FSL. Cluster thresholding was performed via the randomise tool in FSL ($t > 2.0555$, 10000 permutations; the cluster forming threshold was the t-score corresponding to a FWER of 0.05 at 26 degrees of freedom) using probability masks derived from the Harvard-Oxford cortical and subcortical structural atlases. Local maxima are reported only for clusters larger than 600 voxels. ROIs, regions of interest; TMR, Total Meal Replacement; TD, Typical Diet; BL, baseline of fMRI signal; OFC, orbitofrontal cortex; ACC, anterior cingulate cortex; MFG, middle frontal gyrus; dlPFC, dorsolateral prefrontal cortex; NAcc, nucleus accumbens; PCG, precentral gyrus; NS, not significant; FSL, FMRIB Software Library.

left nucleus accumbens appeared to decrease. This finding suggests that TMR may be enhancing the inhibitory influences of the left dorsolateral frontal cortex (which is known to regulate executive control over ingestion) on fMRI-FCR of the food reward and pleasure-regulating left nucleus accumbens (Berridge, 1996).

The analysis conducted to examine the effects of the two dietary interventions on functional interactions between the right dorsolateral prefrontal cortex and the whole brain did not yield

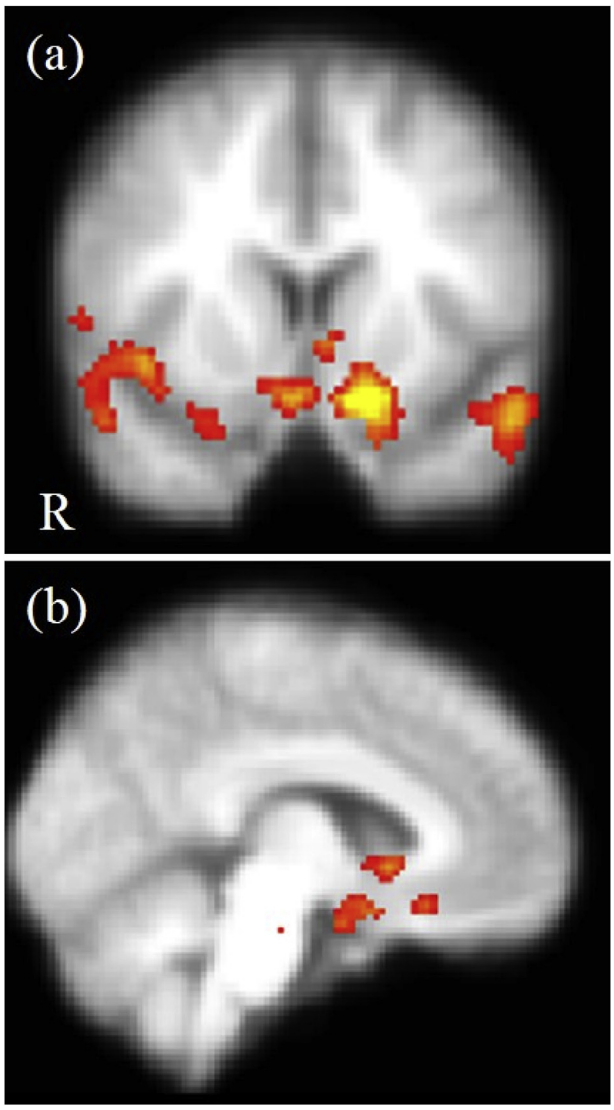

Fig. 3. Brain regions that were negatively modulated post- vs. pre-intervention by the left dlPFC in the TMR group compared to the TD group.
a) Coronal slice of the brain showing significant clusters involving the left NAcc, left subcallosal cortex, left hippocampus and bilateral orbitofrontal cortex.
b) Sagittal slice of the brain showing a significant clusters involving the left nucleus accumbens.
Analyses were conducted using FSL via the PPI approach. Third level random effects models were constructed using the FLAME-1 algorithm in FSL. Cluster thresholding was performed via the randomise tool in FSL ($t > 2.0555$, 10000 permutations). Only the clusters and the local maxima that survived the FWE cluster correction ($P < 0.05$) are shown. The template image is the mean image of the high-resolution anatomical scans of all subjects. TMR, Total Meal Replacement; TD, Typical Diet; dlPFC, dorsolateral prefrontal cortex; NAcc, nucleus accumbens; FSL, FMRIB Software Library; PPI, psychophysiological interaction.

significant findings. In the analyses conducted using probability masks of pre-hypothesized ROIs, significant negative functional interactions were noted between the activity of the right dorsolateral prefrontal cortex and the fMRI-FCR of the left and right amygdala ($P = 0.005$ and $P = 0.01$ respectively), right insula ($P = 0.045$), left nucleus accumbens ($P = 0.005$) and left orbitofrontal cortex ($P = 0.046$) following the TMR condition compared to the TD condition [Table 4]. Further exploration of these findings indicated that observed significant findings in the bilateral amygdala were driven by significant differences in TMR vs. TD groups in the interaction of the left dorsolateral prefrontal cortex and fMRI-FCR of these target brain regions at the pre-intervention state. However, on visual examination of COPEs [Supplemental Fig. 4], TMR intervention was associated with a greater reduction of fMRI-FCR in the left nucleus accumbens along with increased activity of the right dorsolateral prefrontal cortex. Thus, TMR seems to enhance the inhibitory influences of the left as well as right dorsolateral prefrontal cortices on the nucleus accumbens' food reward regulating response (Berridge, 1996).

Pooled analysis of TMR and TD groups to examine the main effect of time (i.e. post- vs. pre-intervention differences in functional connectivity between the seed regions and the whole brain or pre-hypothesized regions of interest), did not reveal any significant clusters.

The TMR group had significant reductions in mean body weight (4.87 kg, $t = 9.03$, $P < 0.001$, Cohen's $d = 2.33$), BMI (1.68 kg/m^2, $t = 9.06$, $P < 0.001$, Cohen's $d = 2.34$) and BF (2.19 kg, $t = 3.47$, $P = 0.004$, Cohen's $d = 0.90$). The TD also had reductions in mean body weight (2.37 kg, $t = 3.58$, $P = 0.004$, Cohen's $d = 0.99$) and BF (1.64 kg, $t = 4.01$, $P = 0.002$, Cohen's $d = 1.11$). Weight loss and BMI reduction in the TMR group was significantly greater than in the TD group (2.50 kg, $t = 2.92$, $P = 0.007$, Cohen's $d = 1.12$; and 1.24 kg/m^2, $t = 2.78$, $P = 0.013$, Cohen's $d = 1.10$ respectively) [Table 2].

4. Discussion

In this prospective 3-week randomized controlled clinical trial, we examined the effects of isocaloric TMR- and TD-based ECR interventions on fMRI-FCR and food cravings. Our findings showed that fMRI-FCR in the dorsolateral prefrontal cortex was increased in the TMR compared to the TD intervention. This is consistent with previous studies (Rosenbaum et al., 2008) indicating that ECR may be increasing overall executive control over ingestion (Kahathuduwa et al., 2016). Given that the dorsolateral prefrontal cortex is involved in exerting executive control over ingestion (Berthoud, 2002, 2004, 2011), a likely explanation for this finding lies in the fundamental difference in the nature of the interventions. TMR participants had to exert executive control over food stimuli to eliminate all foods to a much greater extent compared with the TD group who ate typical foods. The increased fMRI-FCR in the dorsolateral prefrontal cortex may be reflective of this process. This is supported by the fact that restrained eaters, who are believed to show a persistent pattern of exerting cognitive control over ingestion, also have a high level of dorsolateral prefrontal cortical activity (Burger & Stice, 2011; DelParigi et al., 2007; McCaffery et al., 2009; Sweet et al., 2012).

This was further supported by the results of our functional connectivity analyses. Our results indicate that following the TMR intervention, fMRI-FCR of the left nucleus accumbens appears to negatively interact with the left and right dorsolateral prefrontal cortex, potentially indicating that the activity of the dorsolateral prefrontal cortex is negatively modulating (i.e. suppressing) the fMRI-FCR of the left nucleus accumbens (Friston et al., 1997). Previous studies that utilized PPI to examine neural processing of highly rewarding non-food stimuli have interpreted negative interactions between the dorsolateral prefrontal cortex and fMRI-FCR of the nucleus accumbens as possible inhibitory influences of the dorsolateral prefrontal cortex on the nucleus accumbens (Diekhof & Gruber, 2010). The nucleus accumbens is involved in determining the pleasure, reward, and ultimate motivational salience to ingest (Berridge, 1996). Therefore, in the context of the available literature (Harvey et al., 1993; Martin et al., 2006), and our findings in fMRI data analyses, our results in the functional connectivity analyses suggest that TMR may be suppressing both pleasure and motivational salience of food by supporting increases in executive inhibitory control over the brain regions that regulate pleasure and

Table 4
Local maxima within pre-hypothesized ROIs in the functional connectivity analyses.

Seed Region	Negative PPI	ROI	Cluster Size	MNI Coordinates			Subregions	t	P
				X	Y	Z			
L/dlPFC (MFG)	TMR > TD X Post > Pre	L/Amygdala	216	−24	−2	−22	Left amygdala	3.93	0.004
				−14	−8	−18	Left amygdala	3.31	
		R/Amygdala	134	28	−6	−14	Right amygdala	3.36	0.009
				26	2	−18	Right amygdala	2.83	
				28	2	−24	Right amygdala	2.67	
				26	−14	−12	Right amygdala	2.3	
		L/NAcc	47	−6	14	−2	Left NAcc	3.01	0.018
				−12	12	−12	Left NAcc	2.94	
		L/OFC	448	−16	14	−16	Left medial OFC	5.17	0.01
				−22	28	−16	Left medial OFC	3.65	
				−40	24	−20	Left lateral OFC	3.63	
				−20	22	−16	Left medial OFC	3.62	
				−26	24	−22	Left medial OFC	3.34	
				−30	18	−24	Left lateral OFC	3.12	
				−16	34	−22	Left medial OFC	2.1	
				−34	32	−22	Left lateral OFC	2.1	
	TMR > TD X BL > Pre	L/Amygdala	200	−28	−4	−26	Left amygdala	3.57	0.006
				−12	−6	−20	Left amygdala	2.38	
				−16	−4	−12	Left amygdala	2.37	
		R/Amygdala	109	14	−6	−20	Right amygdala	2.89	0.003
				30	2	−22	Right amygdala	2.89	
				26	2	−22	Right amygdala	2.88	
		L/OFC	277	−16	14	−16	Left medial OFC	3.58	0.01
				−30	18	−24	Left lateral OFC	3.54	
				−42	22	−18	Left lateral OFC	3.4	
				−22	22	−16	Left medial OFC	3.32	
R/dlPFC (MFG)	TMR > TD X Post > Pre	L/Amygdala	187	−24	−4	−18	Left amygdala	3.41	0.005
				−14	−8	−18	Left amygdala	3.35	
		R/Amygdala	127	28	−4	−14	Right amygdala	3.07	0.01
				30	2	−16	Right amygdala	2.75	
				12	−4	−20	Right amygdala	2.45	
				18	−4	−22	Right amygdala	2.32	
				28	2	−26	Right amygdala	2.2	
		R/Insula	154	42	14	−10	Right anterior insula	3.18	0.045
				34	10	−14	Right anterior insula	2.77	
				40	20	−2	Right anterior insula	2.45	
				46	4	−2	Right anterior insula	2.29	
		L/NAcc	69	−6	14	−2	Left NAcc	3.35	0.005
				−12	12	−10	Left NAcc	3.14	
		L/OFC	171	−16	14	−18	Left medial OFC	4.12	0.046
				−18	10	−22	Left medial OFC	3.65	
				−20	32	−14	Left medial OFC	2.88	
	TMR > TD X BL > Pre	L/Amygdala	141	−24	0	−16	Left amygdala	2.79	0.012
				−28	−2	−24	Left amygdala	2.5	
				−18	−4	−12	Left amygdala	2.49	
				−14	−8	−18	Left amygdala	2.35	
		R/Amygdala	79	16	−4	−20	Right amygdala	2.78	0.029
				18	2	−18	Right amygdala	2.65	
				30	2	−18	Right amygdala	2.6	
		L/OFC	200	−30	18	−28	Left lateral OFC	3.59	0.028
				−18	14	−16	Left medial OFC	3.29	
				−14	12	−16	Left medial OFC	3.27	
				−40	20	−18	Left lateral OFC	2.66	
				−20	20	−16	Left medial OFC	2.58	
				−38	20	−10	Left lateral OFC	2.27	

Fifteen TMR and 13 TD subjects were included in the analyses. Analyses were conducted using FSL. Third level random effects models were constructed using the FLAME-1 algorithm in FSL. Cluster thresholding was performed via the randomise tool in FSL ($t > 2.0555$, 10000 permutations; the cluster forming threshold was the t-score corresponding to a FWER of 0.05 at 26 degrees of freedom) using probability masks derived from the Harvard-Oxford cortical and subcortical structural atlases. ROIs, regions of interest; TMR, Total Meal Replacement; TD, Typical Diet; BL, baseline of fMRI signal; OFC, orbitofrontal cortex; dlPFC, dorsolateral prefrontal cortex; MFG, middle frontal gyrus; NAcc, nucleus accumbens; FSL, FMRIB Software Library.

reward of food. In addition to increasing suppressive influences of the dorsolateral prefrontal cortex on fMRI-FCR of the nucleus accumbens, our findings also indicated that TMR may be associated with enhancing the negative modulatory effects of the dorsolateral prefrontal cortex on the left orbitofrontal cortex, right insula and bilateral amygdala. Given that these brain regions are also regulating food reward and pleasure associated with ingestion (Berridge, 1996, 2009; Berthoud, 2011), it is reasonable to interpret the present results as suggesting that TMR has enhanced the inhibitory influences of the bilateral dorsolateral prefrontal cortex on hedonic motivational influences to ingest. Further research is needed however to delineate precisely what aspects of the TMR intervention are contributing to these observed outcomes.

For the analysis of fMRI data, we hypothesized based on prior studies (Bruce et al., 2014; Murdaugh et al., 2012; Rosenbaum et al., 2008) that fMRI-FCR of the nucleus accumbens, insula, orbitofrontal and anterior cingulate cortices, which process food reward (Berridge, 2009; Berthoud, 2002, 2011), and the precentral gyrus,

which may be involved in determining motor readiness to ingest (Kahathuduwa et al., 2016), would decrease in TMR versus TD. While the functional connectivity findings were supportive of reductions in fMRI-FCR of at least the nucleus accumbens, insula and the orbitofrontal cortex, in the fMRI analyses these regions showed increased activations. It is notable, however, that none of the previous studies upon which our hypotheses were based directly compared the neurophysiological effects of TMR versus TD interventions. Thus, our finding provides the first direct evidence of the differential impact of diet type on brain fMRI-FCR. Specifically, the observed TMR > TD contrast in the orbitofrontal and anterior cingulate cortices is likely due to an increase in food reward expectation with the TMR intervention, based in the complete absence of typical food ingestion. In other words, when eliminating food completely, the salience of expected reward associated with foods may increase. Conversely the participants in the TD group, who engaged with typical foods throughout the intervention, may not have experienced a similar heightening of relative food reward expectation. Further supporting this theory is the finding that the TD group also showed reductions in at least some constructs that measure food cravings, possibly as a result of a relative reduction in food-cue reactivity in the reward-related regions. However, as suggested by the outcomes of the functional connectivity analyses, implementation of the TMR intervention for a longer duration may plausibly lead to a reversal of the increased fMRI-FCR we observed in the nucleus accumbens and the orbitofrontal cortex via ongoing executive control and consequent deconditioning of food cues relative to reward.

Finally, both TMR and TD interventions resulted in weight loss with the TMR intervention having more than twice the weight loss compared to TD. By controlling for body fat mass in the primary fMRI analysis we were able to observe differential brain influences related to the type of diet somewhat independently of their respective influences on body fat loss. In effect we could better understand how typical food versus stimulus narrowed sources of nutrition (i.e. shakes) may arrive at the observed outcomes. Given our findings, it is likely that weight losses observed in the TMR versus TD condition may in part be achieved through increased executive control over ingestion despite heightened reactivity to visual food cues. These findings appear to reflect neurocognitive changes that are distinct from participants' explicit intentions to regulate food intake.

This study represents the first prospective comparison of the neurophysiological effects of ECR by TMR versus TD in a prospective RCT. Furthermore, to the best of our knowledge, our study represents the first examination of the effects of extended calorie restriction and also the first comparison of the effects of different methods of calorie restriction (i.e. TMR and TD) on task-related functional connectivity between brain regions that regulate ingestive behavior. A further strength is that unlike many fMRI-FCR studies, adequately controlling for the variability introduced by menstrual cyclical hormonal variations eliminates a significant confound. Other strengths include using an isocaloric intervention as the active control and controlling for the duration of pre-scan fasting. In addition, by including change in BF as a function of pre-intervention BF in our models, we were able to draw inferences related to type of diet (as opposed to a non-specific weight loss effect). Additionally, our image bank included a full reward spectrum for food and object images (high through low appeal) and all images were matched for color, shape, visual complexity and overall appearance. This allowed us to experimentally minimize extraneous neural activations related to visual stimulus processing and also generalized reward. Finally, we used a permutation-based non-linear approach, which is robust to the recently outlined limitations (Cornier, Melanson, Salzberg, Bechtell, & Tregellas, 2012) of the Gaussian random field theory-based fMRI analysis pipelines (Kessler, Angstadt, & Sripada, 2016).

Caution is warranted when interpreting some interactions in fMRI and functional connectivity analyses. For instance, differences in fMRI-FCR were noted between the TMR and TD groups at the pre-intervention state in several brain regions (e.g. bilateral dorsolateral prefrontal cortex, right precentral gyrus; Supplemental Fig. 3). Similarly, TMR versus TD differences were observed in the pre-intervention state in the functional connectivity between the left dorsolateral prefrontal cortex and several brain regions (e.g. bilateral amygdala, left orbitofrontal cortex). While this is an important limitation, given the pre-post nature of our design, in the analyses subjects act as their own control, which likely limits the potential for this to substantially influence interpretation.

Our study had some limitations. First, subjects were scanned during both mornings and afternoons. This may have introduced some variability in the fMRI data due to diurnal variations in food-cue reactivity. Second, we did not include a no-intervention control group. Including a free living control group would have allowed us to more directly consider the relative contribution of weight loss to our findings. However, including body fat change in our modeling served as a reasonable surrogate. Third, literature indicates that acute as well as long-term overfeeding and exercise may influence fMRI-FCR (Cornier, Von Kaenel, Bessesen, & Tregellas, 2007, 2009, 2012); in our study design, we could not fully account for these potential confounders; as such this is a limitation. Finally, our food-cue reactivity task required subjects to rate each image using a hand-held device. While this task ensured that the subjects actively attended to and processed stimuli, given that the subjects arrived at a decision and performed a motor response, there may be neurophysiological influences related to this that cannot be accounted for in our design.

In conclusion, following the 3-week intervention, food-cue reactivity in brain regions that 1) regulate food reward (i.e. orbitofrontal cortex, anterior cingulate cortex, insula and nucleus accumbens), 2) are likely to determine motor readiness to ingest (i.e. the primary motor cortex), and 3) exert executive control over ingestion (i.e. the dorsolateral prefrontal cortex) increased in TMR as compared to TD. Our findings as a whole suggest that this is most likely reflective of increased executive control in response to increased fMRI-FCR in brain regions regulating food reward and incentive driven salience towards ingestion by the bilateral dorsolateral prefrontal cortex in the TMR condition as compared to the TD condition when visual food cues are presented. It is plausible that this TMR-associated increase in executive control may have manifested clinically as weight loss and a reduction in overall food cravings.

Conflict of interest statement

The study was funded by Nestlé Health Science Inc. The funding agency was not involved in decisions related to the publication of outcomes. The authors have no other potential conflicts of interest to declare.

Patents

Methods that reduce food cravings, promote weight loss, and/or treat overweight or obesity. Patent application has been filed under No 62/401568 on 29.09.2016 in United States of America.

Sources of support

The study was funded by Nestlé Health Science Inc.

Clinical trials registry number

NCT02637271; the protocol is available at https://clinicaltrials.gov/ct2/show/NCT02637271.

Acknowledgements

The authors wish to thank Blake Johns and Macy Stearns for helping with screening subjects and the staff at the Texas Tech Neuroimaging Institute for their essential role in collecting neuroimaging data.

Appendix A. Supplementary data

Supplementary data related to this article can be found at https://doi.org/10.1016/j.appet.2017.09.025.

References

Andersson, J. L., Jenkinson, M., & Smith, S. (2007). *Non-linear registration, aka Spatial normalisation FMRIB technical report TR07JA2*. FMRIB Analysis Group of the University of Oxford.

Avena, N. M., Murray, S., & Gold, M. S. (2013). Comparing the effects of food restriction and overeating on brain reward systems. *Experimental Gerontology, 48*(10), 1062–1067.

Beckmann, C. F., Jenkinson, M., & Smith, S. M. (2003). General multilevel linear modeling for group analysis in FMRI. *Neuroimage, 20*(2), 1052–1063.

Berridge, K. C. (1996). Food reward: Brain substrates of wanting and liking. *Neuroscience & Biobehavioral Reviews, 20*(1), 1–25.

Berridge, K. C. (2009). 'Liking' and 'wanting' food rewards: Brain substrates and roles in eating disorders. *Physiol Behav, 97*(5), 537–550.

Berthoud, H.-R. (2002). Multiple neural systems controlling food intake and body weight. *Neuroscience & Biobehavioral Reviews, 26*(4), 393–428.

Berthoud, H.-R. (2004). Neural control of appetite: Cross-talk between homeostatic and non-homeostatic systems. *Appetite, 43*(3), 315–317.

Berthoud, H.-R. (2011). Metabolic and hedonic drives in the neural control of appetite: Who is the boss? *Current Opinion in Neurobiology, 21*(6), 888–896.

Bruce, A. S., Bruce, J. M., Ness, A. R., Lepping, R. J., Malley, S., Hancock, L., et al. (2014). A comparison of functional brain changes associated with surgical versus behavioral weight loss. *Obesity (Silver Spring), 22*(2), 337–343.

Burger, K. S., & Stice, E. (2011). Relation of dietary restraint scores to activation of reward-related brain regions in response to food intake, anticipated intake, and food pictures. *Neuroimage, 55*(1), 233–239.

Cornier, M. A., Melanson, E. L., Salzberg, A. K., Bechtell, J. L., & Tregellas, J. R. (2012). The effects of exercise on the neuronal response to food cues. *Physiology & Behavior, 105*(4), 1028–1034.

Cornier, M. A., Salzberg, A. K., Endly, D. C., Bessesen, D. H., Rojas, D. C., & Tregellas, J. R. (2009). The effects of overfeeding on the neuronal response to visual food cues in thin and reduced-obese individuals. *PLoS One, 4*(7), e6310.

Cornier, M. A., Von Kaenel, S. S., Bessesen, D. H., & Tregellas, J. R. (2007). Effects of overfeeding on the neuronal response to visual food cues. *Am J Clin Nutr, 86*(4), 965–971.

Dale, A. M., Fischl, B., & Sereno, M. I. (1999). Cortical surface-based analysis. I. Segmentation and surface reconstruction. *Neuroimage, 9*(2), 179–194.

Deichmann, R., Gottfried, J. A., Hutton, C., & Turner, R. (2003). Optimized EPI for fMRI studies of the orbitofrontal cortex. *Neuroimage, 19*(2 Pt 1), 430–441.

DelParigi, A., Chen, K., Salbe, A. D., Hill, J. O., Wing, R. R., Reiman, E. M., et al. (2007). Successful dieters have increased neural activity in cortical areas involved in the control of behavior. *International Journal of Obesity, 31*(3), 440–448.

Diekhof, E. K., & Gruber, O. (2010). When desire collides with reason: Functional interactions between anteroventral prefrontal cortex and nucleus accumbens underlie the human ability to resist impulsive desires. *Journal of Neuroscience, 30*(4), 1488–1493.

Finer, N. (2001). Low-calorie diets and sustained weight loss. *Obesity Research, 9*(S11), 290S–4S.

Fischl, B., Salat, D. H., van der Kouwe, A. J., Makris, N., Ségonne, F., Quinn, B. T., et al. (2004). Sequence-independent segmentation of magnetic resonance images. *Neuroimage, 23*(Suppl 1), S69–S84.

Franz, M. J., VanWormer, J. J., Crain, A. L., Boucher, J. L., Histon, T., Caplan, W., et al. (2007). Weight-loss outcomes: A systematic review and meta-analysis of weight-loss clinical trials with a minimum 1-year follow-up. *Journal of The American Dietetic Association, 107*(10), 1755–1767.

Friston, K., Buechel, C., Fink, G., Morris, J., Rolls, E., & Dolan, R. (1997). Psychophysiological and modulatory interactions in neuroimaging. *Neuroimage, 6*(3), 218–229.

Harvey, J., Wing, R. R., & Mullen, M. (1993). Effects on food cravings of a very low calorie diet or a balanced, low calorie diet. *Appetite, 21*(2), 105–115.

Jenkinson, M., Bannister, P., Brady, M., & Smith, S. (2002). Improved optimization for the robust and accurate linear registration and motion correction of brain images. *Neuroimage, 17*(2), 825–841.

Jenkinson, M., & Smith, S. (2001). A global optimisation method for robust affine registration of brain images. *Medical Image Analysis, 5*(2), 143–156.

Kahathuduwa, C. N., Boyd, L. A., Davis, T., O'Boyle, M., & Binks, M. (2016). Brain regions involved in ingestive behavior and related psychological constructs in people undergoing calorie restriction. *Appetite, 107*, 348–361.

Kessler, D., Angstadt, M., & Sripada, C. (2016). *Which findings from the functional neuromaging literature can we trust?*. arXiv preprint arXiv:160801274.

Martin, C. K., O'Neil, P. M., & Pawlow, L. (2006). Changes in food cravings during low-calorie and very-low-calorie diets. *Obesity, 14*(1), 115–121.

Martin, C. K., Rosenbaum, D., Han, H., Geiselman, P. J., Wyatt, H. R., Hill, J. O., et al. (2011). Change in food cravings, food preferences, and appetite during a low-carbohydrate and low-fat diet. *Obesity (Silver Spring), 19*(10), 1963–1970.

McCaffery, J. M., Haley, A. P., Sweet, L. H., Phelan, S., Raynor, H. A., Del Parigi, A., et al. (2009). Differential functional magnetic resonance imaging response to food pictures in successful weight-loss maintainers relative to normal-weight and obese controls. *The American Journal of Clinical Nutrition, 90*(4), 928–934.

Murdaugh, D. L., Cox, J. E., Cook, E. W., 3rd, & Weller, R. E. (2012). fMRI reactivity to high-calorie food pictures predicts short- and long-term outcome in a weight-loss program. *Neuroimage, 59*(3), 2709–2721.

Ng, M., Fleming, T., Robinson, M., Thomson, B., Graetz, N., Margono, C., et al. (2014). Global, regional, and national prevalence of overweight and obesity in children and adults during 1980-2013: A systematic analysis for the global burden of disease study 2013. *Lancet, 384*(9945), 766–781.

Rorden, C., & Brett, M. (2000). Stereotaxic display of brain lesions. *Behavioural Neurology, 12*(4), 191–2000.

Rosenbaum, M., Sy, M., Pavlovich, K., Leibel, R. L., & Hirsch, J. (2008). Leptin reverses weight loss-induced changes in regional neural activity responses to visual food stimuli. *The Journal of Clinical Investigation, 118*(7), 2583–2591.

Siegel, J. S., Power, J. D., Dubis, J. W., Vogel, A. C., Church, J. A., Schlaggar, B. L., et al. (2014). Statistical improvements in functional magnetic resonance imaging analyses produced by censoring high-motion data points. *Human Brain Mapping, 35*(5), 1981–1996.

Smith, S. M. (2002). Fast robust automated brain extraction. *Human Brain Mapping, 17*(3), 143–155.

Sweet, L. H., Hassenstab, J. J., McCaffery, J. M., Raynor, H. A., Bond, D. S., Demos, K. E., et al. (2012). Brain response to food stimulation in obese, normal weight, and successful weight loss maintainers. *Obesity (Silver Spring), 20*(11), 2220–2225.

Team, R. C. (2016). *R: A language and environment for statistical computing*. Vienna, Austria: R Foundation for Statistical Computing, 3.2.4 ed.

White, M. A., Whisenhunt, B. L., Williamson, D. A., Greenway, F. L., & Netemeyer, R. G. (2002). Development and validation of the food-craving inventory. *Obesity Research, 10*(2), 107–114.

WHO. (2001). World Medical Association Declaration of Helsinki. Ethical principles for medical research involving human subjects. *Bulletin of the World Health Organization, 79*(4), 373–374.

Woolrich, M. (2008). Robust group analysis using outlier inference. *Neuroimage, 41*(2), 286–301.

Woolrich, M. W., Behrens, T. E., Beckmann, C. F., Jenkinson, M., & Smith, S. M. (2004). Multilevel linear modelling for FMRI group analysis using Bayesian inference. *Neuroimage, 21*(4), 1732–1747.

Woolrich, M. W., Ripley, B. D., Brady, M., & Smith, S. M. (2001). Temporal autocorrelation in univariate linear modeling of FMRI data. *Neuroimage, 14*(6), 1370–1386.